Pulse Distortions Due to Third-Order Dispersion and Dispersion Mismatches in a Phase-Modulator-Based Temporal Pulse Shaping System

Ze Li, Hao Chi, Xianmin Zhang, and Jianping Yao, *Senior Member, IEEE, Fellow, OSA*

***Abstract*—An analysis on pulse distortions due to the third-order dispersion (TOD) and dispersion mismatches in a phase-modulator- (PM) based temporal pulse shaping (TPS) system for the generation of a repetition-rate-multiplied pulse burst is performed. We demonstrate that the profile of a repetition-rate-multiplied pulse burst and the shape of the individual pulses in the pulse burst are distorted due to the TOD and the dispersion mismatches of the dispersive elements. The tolerance of the system to the TOD and the dispersion mismatches when employing an input optical pulse with different pulsewidth is studied. A technique to use predistortion of the RF modulation signal to tackle the pulse distortions is discussed.**

***Index Terms*—Arbitrary waveform generation (AWG), Fourier transform, pulse repetition rate multiplication (PRRM), temporal pulse shaping (TPS).**

I. Introduction

SIGNIFICANT efforts have been made in the past few years to achieve optical pulse repetition rate multiplication (PRRM), which can find many potential applications in high-speed optical communications, radar and modern instrumentation [1]–[4]. Various techniques have been proposed to implement PRRM in the optical domain. Among the numerous techniques, PRRM based on linear filtering using a spectrally periodic filter is considered one of the most promising solutions. In general, linear filtering can be realized by periodic amplitude-only filtering [5]–[9], periodic phase-only filtering [9]–[15], or the combination of the two [16]. Periodic amplitude-only filtering can be achieved using an arrayed-waveguide grating [5], a Fabry–Pérot etalon [6], uniform fiber Bragg gratings (FBGs) [7], superimposed uniform or chirped FBGs [8], [9], or a sampled FBG [10]. Since phase-only filtering could achieve much higher power efficiency than amplitude-only filtering, the implementation of PRRM based on phase-only filtering has been a topic of interest recently. For example, periodic phase-only filtering using a single all-pass optical cavity has been proposed to realize optical PRRM [11]. The method based on temporal self-imaging effect using a linearly chirped FBG (LCFBG) has also been proposed and demonstrated [12], [13].

The major limitation of the techniques in [5]–[13] is that the systems are not reconfigurable. Once the systems are implemented, the temporal features of the pulse burst, such as the repetition rate and the pulse burst profile, are determined, which are not tunable. A solution to the problem is to use a phase-only spatial light modulator (SLM) [14]. Since an SLM can be updated in real time, an SLM-based phase-only filter can be made reconfigurable and the temporal features of the pulse burst can be tunable. The major drawback of an SLM-based system is the bulkiness and complexity. In addition, the coupling between fiber-to-space and space-to-fiber increases the system loss. To solve these problems, an all-fiber based temporal pulse shaping (TPS) system that is reconfigurable for the generation of high-repetition-rate optical pulse bursts was proposed and demonstrated [15]. In the system, a phase modulator (PM) was employed to which a periodic RF modulation signal was applied. The generation of an optical pulse burst with a repetition rate as high as 113 GHz was demonstrated. Since the individual pulse in the pulse burst has an ultra-narrow width, it was hard to be directly observed using an oscilloscope. In [15], the generated pulse burst was observed using an autocorrelator. It is known that the autocorrelation of a pulse or signal does not reveal all the information of the pulse or signal and the distortions due to the third-order dispersion (TOD) and dispersion mismatches were not observed.

In this paper, we perform a detailed analysis on the impact of the TOD and dispersion mismatches on the distortions of the generated pulse burst in a PM-based TPS system for PRRM. A theoretical model is developed, from which pulse distortions due to the TOD and dispersion mismatches are evaluated. Numerical simulations are then performed. Waveform distortions due to the TOD and dispersion mismatches are observed. The tolerance of the system to the TOD and the dispersion mismatches when employing an input optical pulse with different pulsewidth is also evaluated. The predistortion of the RF modulation signal to tackle pulse distortions due to pulse broadening resulted from the TOD is discussed.

Manuscript received April 13, 2010; revised July 21, 2010, August 14, 2010; accepted August 17, 2010. Date of publication August 23, 2010; date of current version September 22, 2010. This work was supported in part by the Natural Sciences and Engineering Research Council of Canada (NSERC). The work of Z. Li was supported by a scholarship from the China Scholarship Council. The work of H. Chi was supported by the National Natural Science Foundation of China (60871011).

Z. Li is with the Microwave Photonics Research Laboratory, School of Information Technology and Engineering, University of Ottawa, Ottawa, ON K1N 6N5, Canada, and also with the Department of Information Science and Electronic Engineering, Zhejiang University, Hangzhou 310027, China.

J. Yao is with the Microwave Photonics Research Laboratory, School of Information Technology and Engineering, University of Ottawa, Ottawa, ON, K1N 6N5, Canada (e-mail: jpyao@site.uOttawa.ca).

H. Chi and X. Zhang are with the Department of Information Science and Electronic Engineering, Zhejiang University, Hangzhou 31002,7 China.

Color versions of one or more of the figures in this paper are available online at http://ieeexplore.ieee.org.

Digital Object Identifier 10.1109/JLT.2010.2069553

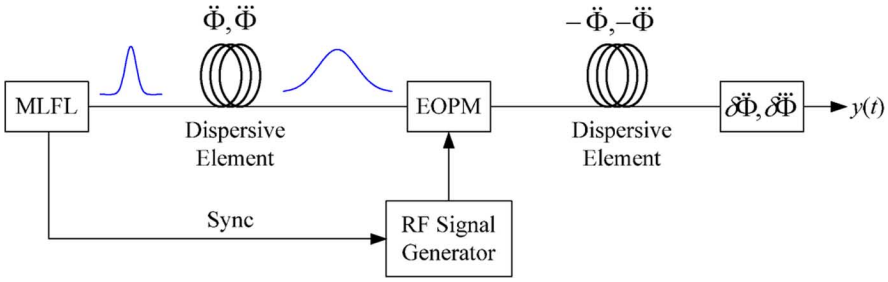

Fig. 1. Schematic of a PM-based TPS system (MLFL: mode-locked fiber laser; EOPM: electro-optic phase modulator).

II. Theoretical Analysis

The schematic of a PM-based TPS system for PRRM is shown in Fig. 1. The system consists of a mode-locked fiber laser (MLFL), two conjugate dispersive elements, and a PM that is connected between the two dispersive elements. A periodic RF modulation signal generated by a microwave signal generator is applied to the PM through the RF port. The phase modulation here corresponds to the periodic phase-only filtering. Since the output pulse could not be directly observed on an oscilloscope, it was observed using an autocorrelator [15]. However, the distortions due to the TOD and the dispersion mismatches were not seen. We will show, based on our analysis, that the profile of a repetition-rate-multiplied pulse burst and the individual pulses in the pulse burst are both distorted due to the TOD and the dispersion mismatches in the dispersive elements.

In the analysis, the average group delay from the dispersive elements, which will only introduce a constant time delay to the generated pulse burst, is ignored. Usually, a dispersive element is a length of dispersive fiber; therefore, the group velocity dispersion (GVD) and the TOD are given by $\ddot{\Phi} = \beta_2 z$ and $\dddot{\Phi} = \beta_3 z$, where z is the length of the dispersive fiber, and $\beta_2 = d^2\beta/d\omega^2$ and $\beta_3 = d^3\beta/d\omega^3$, where β is the propagation constant and ω is the optical angular frequency. The dispersion mismatches between the two dispersive elements are denoted as $\delta\ddot{\Phi}$ and $\delta\ \dddot{\Phi}$, as indicated in Fig. 1.

An input periodic RF modulation signal $s(t)$ with an angular frequency of ω_{RF} is applied to the PM via the RF port. The phase modulation function is given by $x(t) = \exp[jms(t)]$, where m is the modulation index, which is also periodic and can be developed in a Fourier series,

$$x(t) = \sum_{k=-\infty}^{+\infty} a_k \exp(jk\omega_{\mathrm{RF}}t) \tag{1}$$

where $a_k = (1)/(T)\int_T e^{jms(t)} \cdot e^{-jk\omega_{\mathrm{RF}}t}dt$ is the k-th order Fourier series coefficient and T is the period of the modulation signal. Thus, the Fourier transform (FT) of $x(t)$ can be expressed as

$$\tilde{X}(\omega) = 2\pi \sum_{k=-\infty}^{+\infty} a_k \delta(\omega - k\omega_{\mathrm{RF}}) \tag{2}$$

where $\delta(t)$ is the Dirac delta function.

The transfer functions of the two conjugate dispersive elements without considering the dispersion mismatches are given by

$$H_{\ddot{\Phi}+\dddot{\Phi}} = \exp\left[-j\left(\frac{\ddot{\Phi}\omega^2}{2} + \frac{\dddot{\Phi}\,\omega^3}{6}\right)\right] \tag{3}$$

and

$$H_{-\ddot{\Phi}-\dddot{\Phi}} = \exp\left[j\left(\frac{\ddot{\Phi}\omega^2}{2} + \frac{\dddot{\Phi}\,\omega^3}{6}\right)\right] \tag{4}$$

Assume that the input ultrashort optical pulse $g(t)$ is transform-limited and its Fourier transform is $\tilde{G}(\omega)$, the output signal at the output of the second dispersive element is then given by

$$\tilde{Y}(\omega) = \left\{\frac{1}{2\pi}\left[\tilde{G}(\omega)H_{\ddot{\Phi}+\dddot{\Phi}}\right] * \tilde{X}(\omega)\right\} \cdot H_{-\ddot{\Phi}-\dddot{\Phi}} \tag{5}$$

where $*$ denotes the convolution operation. Substituting (2), (3) and (4) into (5), we can obtain (6), shown at the bottom of the following page, where Ω is the integration variable, and the corresponding time-domain expression is given by

$$y(t) = \sum_{k=-\infty}^{+\infty} \left\{ \begin{array}{l} a_k \times \exp\left[-j\frac{1}{6}(3\ddot{\Phi} + \dddot{\Phi}\ k\omega_{\mathrm{RF}}) \cdot (k\omega_{\mathrm{RF}})^2\right] \\ \quad \times \exp[j(\omega_c + k\omega_{\mathrm{RF}})t] \\ \quad \times g\left[t - \ddot{\Phi} \cdot k\omega_{\mathrm{RF}} - \frac{1}{2}\dddot{\Phi} \cdot (k\omega_{\mathrm{RF}})^2\right] \\ \quad * \exp\left(j\frac{t^2}{2\ddot{\Phi}\cdot k\omega_{\mathrm{RF}}}\right) \end{array} \right\} \tag{7}$$

From (7), it can be seen that the periodic phase-only filtering is an operation that spreads an input ultrashort pulse to form a high-repetition-rate pulse burst with each individual pulse in the burst maintaining the same shape as the input ultrashort optical pulse. For each individual pulse, the first term a_k in (7) is a magnitude coefficient and the second term $\exp[-j(1/6)(3\ddot{\Phi} + \dddot{\Phi}\ k\omega_{\mathrm{RF}}) \cdot (k\omega_{\mathrm{RF}})^2]$ is a constant phase term. These two terms are independent of time. The third term $\exp[j(\omega_c + k\omega_{\mathrm{RF}})t]$ indicates that the central frequency of the k-th pulse is shifted from ω_c to $\omega_c + k\omega_{\mathrm{RF}}$, but this shift will not change the shape of the pulse. The fourth term $g[t - \ddot{\Phi} \cdot k\omega_{\mathrm{RF}} - (1/2)\ \dddot{\Phi} \cdot (k\omega_{\mathrm{RF}})^2]$ shows that the k-th optical pulse is shifted by $\ddot{\Phi} \cdot k\omega_{\mathrm{RF}} + (1/2)\ \dddot{\Phi} \cdot (k\omega_{\mathrm{RF}})^2$. Thus, the interval between two adjacent pulses could be tuned by changing the period of the RF modulation signal.

The impact of the TOD on the pulse distortions can be observed from the fourth term. The presence of the TOD introduces an additional temporal shift to each pulse, which is $\dddot{\Phi}\cdot(k\omega_{\rm RF})^2/2$. Compared with the term $\ddot{\Phi}\cdot k\omega_{\rm RF}$, the TOD-induced temporal shift, $\dddot{\Phi}\cdot(k\omega_{\rm RF})^2/2$, is very small and can be ignored. The major impact that leads to pulse distortions comes from the last term $\exp(j(t^2)/(2\dddot{\Phi}\cdot k\omega_{\rm RF})$, which is a quadratic phase term induced by the TOD. The convolution between the quadratic phase term and an individual pulse in the burst will lead to temporal broadening of the individual pulse and also lead to peak power decrease [17].

Now, we consider the influence of the dispersion mismatches on the distortions of the generated pulse burst. The spectrum of the output waveform, taking into consideration of the dispersion mismatches of $\delta\ddot{\Phi}$ and $\delta\ \dddot{\Phi}$, can be expressed as

$$\begin{aligned}\tilde{Y}(\omega)&=\sum_{k=-\infty}^{+\infty}\left\{\begin{array}{l}a_k\tilde{G}(\omega+k\omega_{\rm RF})\\ \quad\times\exp\left[-j\frac{1}{6}(3\ddot{\Phi}+\dddot{\Phi}\,k\omega_{\rm RF})\cdot(k\omega_{\rm RF})^2\right]\\ \quad\times\exp\left[-j\left(\ddot{\Phi}+\frac{1}{2}\,\dddot{\Phi}\,k\omega_{\rm RF}\right)\cdot k\omega_{\rm RF}\cdot\omega\right]\\ \quad\times\exp\left(-j\frac{1}{2}\,\dddot{\Phi}\cdot k\omega_{\rm RF}\cdot\omega^2\right)\end{array}\right\}\\ &\quad\times\exp\left[-j\left(\frac{\delta\ddot{\Phi}\omega^2}{2}+\frac{\delta\,\dddot{\Phi}\,\omega^3}{6}\right)\right]\end{aligned}\tag{8}$$

From (8), we can see that the influence of the GVD mismatch $(\delta\ddot{\Phi})$ is similar to that of the non-zero TOD, which also leads to temporal broadening of the individual pulses. However, the broadening induced by $\delta\ddot{\Phi}$ is independent of k, which indicates that the mismatch $\delta\ddot{\Phi}$ introduces an identical distortion to all the pulses. For a k-th pulse, the quadratic phase term from $\delta\ddot{\Phi}$ may exactly cancel the quadratic phase term introduced by the TOD when $\dddot{\Phi}\cdot k\omega_{\rm RF}+\delta\ddot{\Phi}=0$ is satisfied, and the k-th pulse can be considered transform limited if the TOD mismatch is small. However, other pulses, including the 0-th pulse, will experience severe temporal broadening, which will make the envelope of the pulse burst asymmetric. The phase term in (8) introduced by the TOD mismatch $\delta\ \dddot{\Phi}$ will lead to distortions to each of the pulses and make each pulse shape asymmetric with an oscillatory structure near one of its edges [18]. Due to the symmetrical nature of autocorrelation operation, the pulse distortions cannot be observed if only the autocorrelation results are recorded, as it was done in [15].

The tolerance of the system to the TOD and the dispersion mismatches is also dependent on the pulsewidth of an input optical pulse. In practice, we are often interested in the extent of the pulse broadening rather than the details of the pulse shape distortions. Thus, in our analysis we use the root-mean-square (RMS) width, σ, to describe the extent of the individual pulse broadening [18]. If the input pulse is assumed to be a transform-limited Gaussian pulse, the pulse broadening factor is given by [18]

$$\frac{\sigma}{\sigma_0}=\left[1+\left(\frac{\dddot{\Phi}\cdot k\omega_{\rm RF}+\delta\ddot{\Phi}}{2\sigma_0^2}\right)^2+\frac{1}{2}\left(\frac{\delta\,\dddot{\Phi}}{4\sigma_0^3}\right)^2\right]^{1/2}\tag{9}$$

where $\sigma_0=T_0/\sqrt{2}$ is the RMS width of the input pulse, T_0 is the half-width at $1/e$ intensity point of the input pulse, and σ is the RMS width of the output pulse. It can be seen from (9) that for a given TOD and dispersion mismatches, an input optical pulse with a larger width will lead to relatively smaller temporal broadening or oscillatory structure to the generated pulse burst. Therefore, the use of a wider input optical pulse would make the system have better tolerance to pulse distortions. As

$$\begin{aligned}\tilde{Y}(\omega)&=\left[\int_{-\infty}^{+\infty}\tilde{X}(\omega-\Omega)\tilde{G}(\Omega)H_{\ddot{\Phi}+\dddot{\Phi}}(\Omega)d\Omega\right]\times H_{-\ddot{\Phi}-\dddot{\Phi}}(\omega)\\ &=\left\{\int_{-\infty}^{+\infty}\left[\sum_{k=-\infty}^{+\infty}a_k\delta(\omega-\Omega+k\omega_{\rm RF})\right]\tilde{G}(\Omega)\exp\left[-j\left(\frac{\ddot{\Phi}\Omega^2}{2}+\frac{\dddot{\Phi}\,\Omega^3}{6}\right)\right]d\Omega\right\}\\ &\quad\times\exp\left[j\left(\frac{\ddot{\Phi}\omega^2}{2}+\frac{\dddot{\Phi}\,\omega^3}{6}\right)\right]\\ &=\tilde{G}(\omega+k\omega_{\rm RF})\times\exp\left\{-j\left[\frac{\ddot{\Phi}(\omega+k\omega_{\rm RF})^2}{2}+\frac{\dddot{\Phi}\,(\omega+k\omega_{\rm RF})^3}{6}\right]\right\}\\ &\quad\times\left\{\int_{-\infty}^{+\infty}\left[\sum_{k=-\infty}^{+\infty}a_k\delta(\omega-\Omega+k\omega_{\rm RF})\right]d\Omega\right\}\times\exp\left[j\left(\frac{\ddot{\Phi}\omega^2}{2}+\frac{\dddot{\Phi}\,\omega^3}{6}\right)\right]\\ &=\sum_{k=-\infty}^{+\infty}\left\{\begin{array}{l}a_k\tilde{G}(\omega+k\omega_{\rm RF})\\ \quad\times\exp\left[-j\frac{1}{6}(3\ddot{\Phi}+\dddot{\Phi}\,k\omega_{\rm RF})\cdot(k\omega_{\rm RF})^2\right]\\ \quad\times\exp\left[-j\left(\ddot{\Phi}+\frac{1}{2}\,\dddot{\Phi}\,k\omega_{\rm RF}\right)\cdot k\omega_{\rm RF}\cdot\omega\right]\\ \quad\times\exp\left(-j\frac{1}{2}\,\dddot{\Phi}\cdot k\omega_{\rm RF}\cdot\omega^2\right)\end{array}\right\}\end{aligned}\tag{6}$$

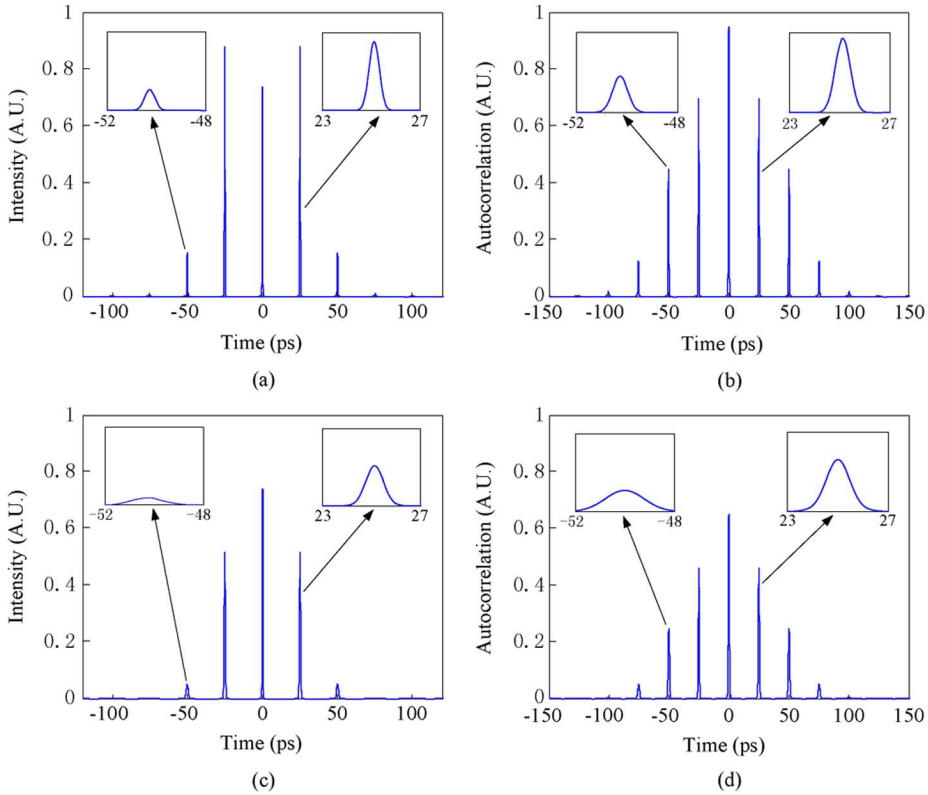

Fig. 2. Optical burst generation using a TPS system without and with considering the TOD. (a) Output pulse burst with two conjugate dispersive elements having only the GVD. (b) Autocorrelation of the optical burst in (a). (c) Output optical pulse burst with two conjugate dispersive elements having both the GVD and TOD. (d) Autocorrelation of the optical pulse burst in (c). Insets: zoom-in views of the corresponding pulses.

the temporal broadening and the oscillatory structure would result in pulse overlap in the burst, especially when the pulse repetition rate is high, the distortions due to the TOD and dispersion mismatches will restrict the highest multiplication factor of the system. Thus, the input pulsewidth should be chosen appropriately in a practical system.

III. Numerical Results

To verify the theoretical analysis, numerical simulations are performed. A transform-limited Gaussian pulse centered at 1550 nm with a full-width at half-maximum (FWHM) of 500 fs is used as the input optical pulse. The GVD of the first dispersive element is set at 1000 ps^2, which corresponds to a standard single-mode fiber (SSMF) of about 50-km as $\beta_2 \approx 20$ ps^2/km at the wavelength of 1550 nm for SSMF. The second dispersive element has a matching dispersion of -1000 ps^2, which can be a 5-km dispersion-compensating fiber with $\beta_2 \approx 200$ ps^2/km.

In the simulation, the RF modulation signal is a single-frequency microwave tone. The phase modulation function is given by

$$x(t) = \exp[jm\cos(\omega_{\mathrm{RF}}t)] = \sum_{k=-\infty}^{\infty} j^k J_k(m)\exp(jk\omega_{\mathrm{RF}}t) \tag{10}$$

Thus, the k-th order Fourier series coefficient is determined by the k-th order Bessel function of the first kind, $J_k(m)$, where m is again the modulation index, and the output pulse intensity is proportional to $J_k^2(m)$. The microwave frequency is set at 4 GHz and the modulation index $m = 1.5$. Based on (7), the interval between two adjacent pulses is $T_R = \ddot{\Phi}\omega_{\mathrm{RF}}$, which is calculated to be 25.1 ps, corresponding to a repetition rate of 39.8 GHz.

First, we consider an ideal case in which the TOD is zero and the GVDs are perfectly matched, i.e., $\dddot{\Phi} = 0, \delta\ddot{\Phi} = \delta\,\dddot{\Phi} = 0$. The intensity of the output optical burst is shown in Fig. 2(a) and the autocorrelation output is shown in Fig. 2(b). As can be seen, a high-repetition-rate pulse burst with a repetition period of 25.1 ps is obtained and the intensity of the k-th pulse is proportional to $J_k^2(1.5)$, which agree well with our analysis.

Next, we consider the influence of the TOD, i.e., $\dddot{\Phi} \neq 0$ and the GVDs are perfectly matched, i.e., $\delta\ddot{\Phi} = \delta\,\dddot{\Phi} = 0$. In a SSMF at around 1558 nm, $\beta_3 \approx 0.1$ ps^3/km, thus, for a 50-km SSMF, the TOD is about 5 ps^3. The output pulse burst is shown in Fig. 2(c), from which we can see that the pulses in the optical burst are significantly broadened and the envelope of the pulse burst is distorted due to the different power decrease of the individual pulses in the burst. In addition, the broadening is symmetrical to the central pulse and the higher order pulses would experience larger broadening. Note that the extra temporal shifts due to $\dddot{\Phi}$, which are equal to $\dddot{\Phi}\cdot(k\omega_{\mathrm{RF}})^2/2$, are small and could be ignored. These results confirm our theoretical prediction. As a comparison, the autocorrelation output is shown in Fig. 2(d). As can be seen the autocorrelation is similar to that shown in Fig. 2(b), and the pulsewidth change to the individual pulses can be observed from the autocorrelation output in this case,

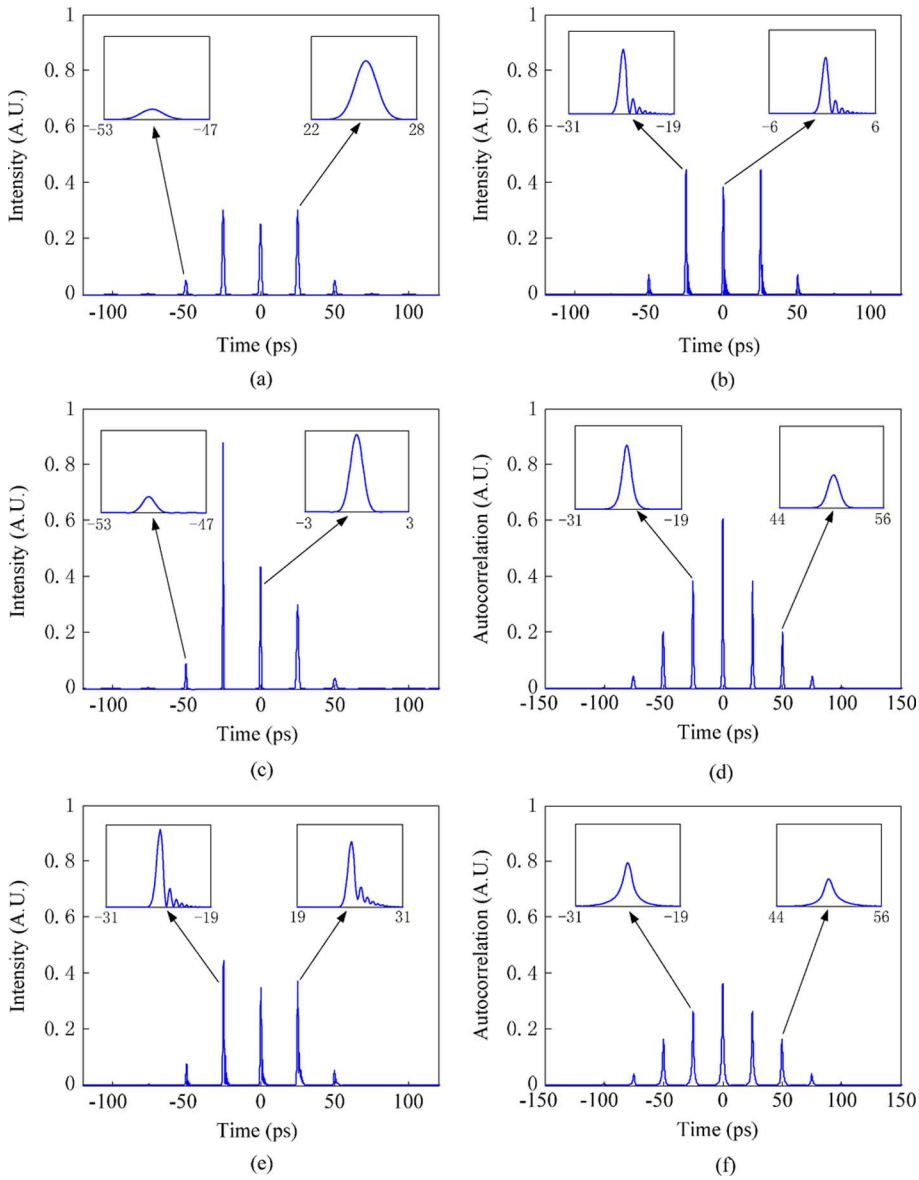

Fig. 3. Optical burst generation using a TPS system having dispersion mismatches. (a) GVD mismatch only, without the TOD. (b) Output pulse burst with the TOD and TOD mismatch, without the GVD mismatch. (c) GVD mismatch to compensate the TOD induced broadening at the -1st-order pulse, without the TOD mismatch. (d) Autocorrelation of the pulse burst in (c). (e) Output pulse burst with the TOD and both the GVD and TOD mismatches. (f) Autocorrelation of the pulse burst in (e). Insets: zoom-in views of the corresponding pulses.

but the distortion to the envelope of the pulse burst due to the TOD cannot be observed.

Then, we study the influence of the dispersion mismatches on the distortions of the generated optical burst. In the simulation, we assume the GVDs are not matched and the TOD is zero ($\ddot{\Phi}= 0$ ps^3, $\delta\ddot{\Phi} = 0.25$ ps^2, $\delta\ \dddot{\Phi}= 0$ ps^3). Fig. 3(a) shows the generated optical burst. The individual pulses in the burst shown in Fig. 3(a) are slightly broadened and the amount of broadening is identical for all pulses, which is similar to the case with the existence of the TOD, as it was indicated in (8), from where we can see that the individual pulses are convolved with a quadratic phase term, leading to pulse broadening. In a practical system, however, the TOD in a SSMF and a DCF can be hardly matched perfectly and we assume a 4% TOD mismatch in our case, which is 0.2 ps^3. Fig. 3(b) shows the simulation result in which the GVDs are perfectly matched but the TODs are not matched, i.e., $\ddot{\Phi}= 5$ ps^3, $\delta\ddot{\Phi} = 0$ ps^2 and $\delta\ \dddot{\Phi}= 0.2$ ps^3. An oscillatory structure at the base of each individual pulse can be clearly observed.

Fig. 3(c) shows the result for a TPS system having both the TOD and the GVD mismatches. In the simulation, we make the amount of the GVD mismatch compensate exactly the broadening due to the TOD on the -1st-order pulse, i.e., $-\ \ddot{\Phi} \cdot\omega_{\mathrm{RF}} + \delta\ddot{\Phi} = 0$, with $\ddot{\Phi}= 5$ ps^3, $\delta\ddot{\Phi} = 0.126$ ps^3, and $\delta\ \dddot{\Phi}= 0$ ps^3. From Fig. 3(c), we can see that the -1st-order pulse become transform-limited, while the other pulses are broadened. The amount of broadening is identical for the pulses that are symmetrically located with respect to this transform-limited pulse. For example, the quadratic phase terms for the -2nd- and 0th-order pulses are $-2\ \ddot{\Phi} \cdot\omega_{\mathrm{RF}} + \delta\ddot{\Phi}$ and $\delta\ddot{\Phi}$, which are opposite but equal in magnitude, the widths of the two broadened pulses are identical, as shown in Fig. 3(c). Fig. 3(d) shows the autocorrelation output of the pulse burst in Fig. 3(c), from which we can see that the asymmetry information is lost due to its symmetric

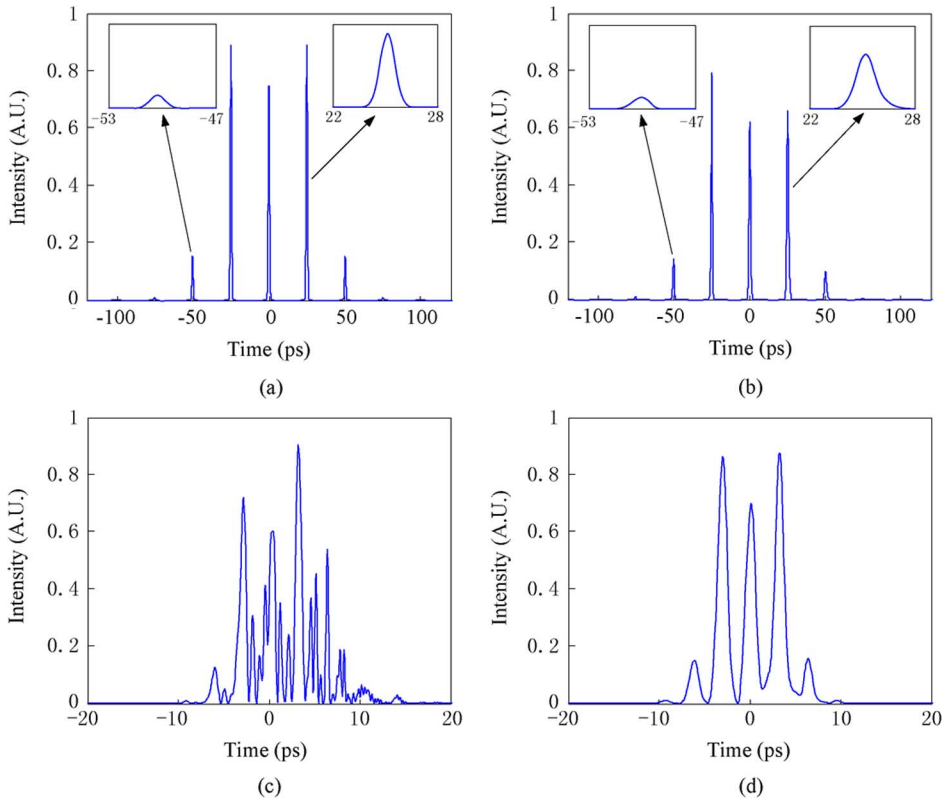

Fig. 4. (a) Generated pulse burst with an input pulsewidth of 1 ps and only matched GVD in the system. Insets: zoom-in views of the 1st-order and −2nd-order pulses. (b) Pulse burst with distortions due to both the TOD and dispersion mismatches. Insets: zoom-in views of the 1st-order and −2nd-order pulses. (c) Pulse burst with a repetition rate of 320 GHz and an input pulsewidth of 300 fs. (d) Pulse burst with a repetition rate of 320 GHz and an input pulsewidth of 1 ps.

nature of autocorrelation operation. The result in Fig. 3(d) is similar to that in Fig. 2(d). Fig. 3(e) shows the output pulse burst when the TOD and both the GVD and TOD mismatches are considered, i.e., $\dddot{\Phi}$= 5 ps^3, $\delta\ddot{\Phi} = 0.25$ ps^2, and $\delta\ \dddot{\Phi}$= 0.2 ps^3. As indicated in (8), both pulse broadening and oscillation would be generated, which can be clearly seen from Fig. 3(e). Fig. 3(f) shows the autocorrelation of the optical pulse burst shown in Fig. 3(e). It is obvious that the oscillatory structure can not be observed from Fig. 3(f). By comparing the results shown in Figs. 2(b), (d) and 3(d), (f), we can conclude that the autocorrelation can be used to estimate the width of the individual pulses but it provides little information about the details of the pulse shape distortions or the pulse burst envelope distortions. Thus, it may not be sufficient to use autocorrelation to characterize the generated pulse burst since some key information is not maintained in the autocorrelation operation. Note that in the simulations, the dispersion mismatches are intentionally set at a larger value to make the distortions more visible.

Finally, we study the tolerance of the PM-based TPS system to pulse broadening for an input optical pulse with different pulse width. To do so, we change the optical pulsewidth from 500 fs to 1 ps and maintain the other parameters unchanged (i.e., $m = 1.5, \ddot{\Phi} = 1000$ ps^2 and $\omega_{\mathrm{RF}} = 4$ GHz). Fig. 4(a) shows the generated pulse burst without the TOD or dispersion mismatches. In Fig. 4(b), a pulse burst with distortions due to the TOD and dispersion mismatches is observed. The parameters are the same as those used for the generation of the pulse burst shown in Fig. 3(c) (i.e., $\dddot{\Phi}$= 5 ps^3, $\delta\ddot{\Phi} = 0.25$ ps^2 and $\delta\ \dddot{\Phi}$= 0.2 ps^3). By comparing Figs. 4(b) and 3(c), we can see that the same amount of the TOD and dispersion mismatches will lead to far less pulse broadening and oscillation to the pulse burst with a wider input optical pulse, which again agrees well with the theoretical analysis. Fig. 4(c) shows a generated pulse burst when the repetition rate of the pulse burst is increased from 40 GHz to 320 GHz (pulse interval reduced from 25.1 ps to 3.125 ps) by decreasing the modulation microwave frequency from 4 GHz to 500 MHz. The optical pulsewidth for Fig. 4(c) is 300 fs and other parameters are kept the same as those used for Fig. 3(c), (i.e., $m = 1.5, \ddot{\Phi} = 1000$ ps^2, $\dddot{\Phi}$= 5 ps^3, $\delta\ddot{\Phi} = 0.25$ ps^2, and $\delta\ \dddot{\Phi}$= 0.2 ps^3). The pulse burst in Fig. 4(c) is distorted severely and the individual pulses can hardly be distinguished. Fig. 4(d) shows a generated pulse burst when the input optical pulsewidth is increased to 1 ps and the other conditions are kept the same as those for Fig. 4(c). We can see that the distortions of each individual pulse and the envelope of the pulse burst in Fig. 4(d) are much smaller than those in Fig. 4(c). As a conclusion, a wider input optical pulse could achieve a higher multiplication factor as long as the input pulsewidth is not too wide to result in pulse overlapping.

IV. Discussion

The pulse burst distortions can be eliminated if the RF modulation signal is properly predistorted. The technique to use predistortion to eliminate the TOD-induced waveform distortion was proposed in [19]. The same concept can also be employed to eliminate the pulse burst broadening due to the TOD in a

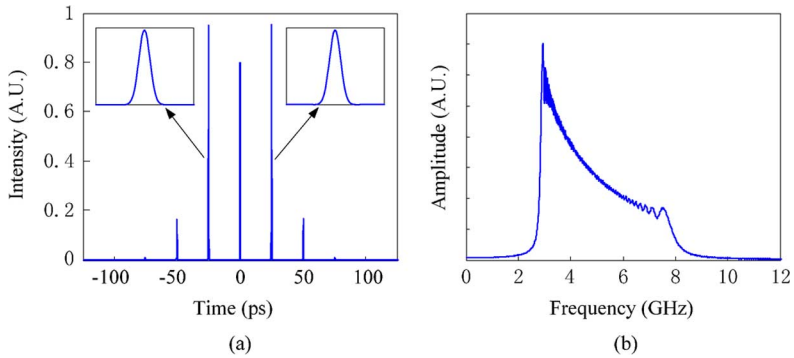

Fig. 5. (a) Pulse burst generated using a predistorted RF modulation signal. Insets: zoom-in views of the −1st-order and 1st-order pulses. (b) Spectrum of the pre-chirped signal.

PM-based TPS system when the input pulse is Gaussian and the conditions $T_0^2/|\ddot{\Phi}| \ll 1$ and $T_0\omega_{\mathrm{RF,max}} \ll 1$, are satisfied, where $\omega_{\mathrm{RF,max}}$ is the maximum angular frequency of the RF modulation signal. According to [19], a predistorted modulation signal can be expressed as

$$w(t) = s\left(\frac{-1+\sqrt{1+2t\,\dddot{\Phi}/\ddot{\Phi}^2}}{\dddot{\Phi}/\ddot{\Phi}^2}\right) \times \begin{cases} t \geq -\ddot{\Phi}^2/(2\,\dddot{\Phi}) & \text{if} \quad \dddot{\Phi} > 0 \\ t \leq -\ddot{\Phi}^2/(2\,\dddot{\Phi}) & \text{if} \quad \dddot{\Phi} < 0 \end{cases} \tag{12}$$

We can see that, the predistorted RF modulation signal is truncated. Here, we use a single tone modulation signal, $\cos(\omega_{\mathrm{RF}}t)$, where ω_{RF} is again the angular frequency of the modulation RF signal, to help understand (12). Based on (12), the predistorted signal is $\cos(\omega_{\mathrm{RF}}(-1+\sqrt{1+2t\,\dddot{\Phi}/\ddot{\Phi}^2})/(\dddot{\Phi}/\ddot{\Phi}^2))$. As $|\ddot{\Phi}^2/(2\,\dddot{\Phi})|$ (100 ns in our case) is usually much larger than the width of the broadened optical pulse after the first dispersive element, based on (12) it is appropriate to assume that the useful predistorted modulation signal is restricted within a time period of $-|\ddot{\Phi}^2/(2\,\dddot{\Phi})| \leq t \leq |\ddot{\Phi}^2/(2\,\dddot{\Phi})|$. Thus, $-1 \leq 2t\,\dddot{\Phi}/\ddot{\Phi}^2 \leq 1$ is satisfied. By applying power series expansion to $\sqrt{1+2t\,\dddot{\Phi}/\ddot{\Phi}^2}$ and ignoring the third and higher-order terms, we obtain the predistorted signal, given by $\cos[(\omega_{\mathrm{RF}} - \omega_{\mathrm{RF}}(\dddot{\Phi})/(2\ddot{\Phi}^2 t))t]$, from which we can see that the predistorted signal can be approximated as a linearly chirped RF signal and the chirp rate is $\omega_{\mathrm{RF}}(\dddot{\Phi}/2\ddot{\Phi}^2)$. If the third and higher-order terms are considered, the predistorted signal is nonlinearly chirped. Fig. 5(a) shows an output pulse burst with a predistorted RF modulation signal, to compensate the temporal broadening induced by the TOD in Fig. 2(c). The generated pulse burst is identical to that shown in Fig. 2(a) and is free of distortion. The spectrum of the predistorted RF modulation signal is shown in Fig. 5(b), which is much more complicated than the 4-GHz RF tone. Therefore, the pulse burst distortion due to the TOD can be eliminated by predistorting the RF modulation signal, but at the cost of a complicated RF generator from which a sophisticated RF modulation signal can be generated. In practice, the GVD and TOD mismatches will also exist in the system and will influence the optical pulse burst generation even when the input optical pulse is predistorted. Since an output optical pulse with predistortion is transformed-limited, the impact from the GVD and TOD mismatches should be similar to that when an optical pulses is propagating in a section of dispersive element: the GVD and TOD mismatches will lead to pulse broadening and asymmetric oscillation to the individual pulses in the pulse burst, respectively. Thus, both the GVD and the TOD should be controlled to be well matched.

V. Conclusion

We have performed a comprehensive investigation on pulse distortions due to the TOD and dispersion mismatches in a PM-based TPS system for the generation of a repetition rate multiplied pulse burst. A theoretical analysis was performed, in which an equation that relates the output pulse burst and the GVD and TOD was developed. Based on the equation, the distortions due to the TOD and the dispersion mismatches were analyzed. Numerical simulations were performed and the results confirmed the theoretical analysis. The tolerance of the PM-based TPS system to distortions for an input optical pulse with different pulsewidth was also analyzed and verified by numerical simulations. The results showed that a wider input optical pulse has a better tolerance to the TOD- and dispersion-mismatch-induced distortions. The use of a predistorted RF modulation signal to compensate the distortion introduced by the TOD was analyzed, and was also verified by numerical simulations.

References

[1] A. M. Weiner, "Femtosecond pulse shaping using spatial light modulators," *Rev. Sci. Instrum.*, vol. 71, no. 5, pp. 1929–1960, May 2000.

[2] P. C. Chou, H. A. Haus, and J. F. Brennan III, "Reconfigurable time-domain spectral shaping of an optical pulse stretched by a fiber Bragg grating," *Opt. Lett.*, vol. 25, no. 8, pp. 524–526, Apr. 2000.

[3] Z. Jiang, C. Huang, D. E. Leaird, and A. M. Weiner, "Spectral line-by-line pulse shaping for optical arbitrary pulse-train generation," *J. Opt. Soc. Amer. B*, vol. 24, no. 9, pp. 2124–2128, Nov. 2007.

[4] J. D. McKinney, D. E. Leaird, and A. M. Weiner, "Millimeter-wave arbitrary waveform generation with a direct space-to-time pulse shaper," *Opt. Lett.*, vol. 27, no. 15, pp. 1345–1347, Aug. 2002.

[5] D. E. Leaird, S. Shen, A. M. Weiner, A. Sugita, S. Kamei, M. Ishii, and K. Okamoto, "Generation of high-repetition-rate WDM pulse trains from an arrayed-waveguide grating," *IEEE Photon. Technol. Lett.*, vol. 13, no. 3, pp. 221–223, Mar. 2001.

[6] K. Yiannopoulos, K. Vyrsokinos, D. Tsiokos, E. Kehayas, N. Pleros, G. Theophilopoulos, T. Houbavlis, G. Guekos, and H. Avramopoulos, "Pulse repetition frequency multiplication with spectral selection in Fabry–Pérot filters," *IEEE J. Quantum Electron.*, vol. 40, no. 2, pp. 157–165, Feb. 2004.
[7] N. K. Berger, B. Levit, S. Atkins, and B. Fischer, "Repetition-rate multiplication of optical pulses using uniform fiber Bragg gratings," *Opt. Commun.*, vol. 221, no. 4–6, pp. 331–335, Jun. 2003.
[8] J. Azaña, P. Kockaert, R. Slavík, L. R. Chen, and S. LaRochelle, "Generation of a 100-GHz optical pulse train by pulse repetition rate multiplication using superimposed fiber Bragg gratings," *IEEE Photon. Technol. Lett.*, vol. 15, no. 3, pp. 413–415, Mar. 2003.
[9] J. Azana, R. Slavik, P. Kockaert, L. R. Chen, and S. LaRochelle, "Generation of customized ultrahigh repetition rate pulse sequences using superimposed fiber Bragg gratings," *J. Lightw. Technol.*,, vol. 21, no. 6, pp. 1490–1498, Jun. 2003.
[10] P. Petropoulos, M. Ibsen, M. N. Zervas, and D. J. Richardson, "Generation of 40-GHz pulse stream by pulse multiplication with a sampled fiber Bragg grating," *Opt. Lett.*, vol. 25, no. 8, pp. 521–523, Apr. 2000.
[11] M. A. Preciado and M. A. Muriel, "Repetition-rate multiplication using a single all-pass optical cavity," *Opt. Lett.*, vol. 33, no. 9, pp. 962–964, May 2008.
[12] J. Azana and M. A. Muriel, "Technique for multiplying the repetition rates of periodic trains of pulses by means of a temporal self-imaging effect in chirped fiber grating," *Opt. Lett.*, vol. 24, no. 23, pp. 1672–1674, Dec. 1999.
[13] S. Atkins and B. Fischer, "All-optical pulse rate multiplication using fractional Talbot effect and field-to-intensity conversion with cross-gain modulation," *IEEE Photon. Technol. Lett.*, vol. 15, no. 1, pp. 132–134, Jan. 2003.
[14] A. M. Weiner, S. Oudin, D. E. Leaird, and D. H. Reitze, "Shaping of femtosecond pulses using phase-only filters designed by simulated annealing," *J. Opt. Soc. Am. A*, vol. 10, no. 5, pp. 1112–1120, May 1993.
[15] J. Azana, N. K. Berger, B. Levit, and B. Fischer, "Reconfigurable generation of high-repetition-rate optical pulse sequences based on time domain phase-only filtering," *Opt. Lett.*, vol. 30, no. 23, pp. 3228–3230, Dec. 2005.
[16] X. Chen and H. Li, "Simultaneous optical pulse multiplication and shaping based on the amplitude-assisted phase-only filter utilizing a fiber Bragg grating," *J. Lightw. Technol.*, vol. 27, no. 23, pp. 5246–5252, Dec. 2009.
[17] R. E. Saperstein, N. Alic, D. Panasenko, R. Rokitski, and Y. Fainman, "Time-domain waveform processing by chromatic dispersion for temporal shaping of optical pulses," *J. Opt. Soc. Amer. B*, vol. 22, no. 11, pp. 2427–2436, Nov. 2005.
[18] G. P. Agrawal, *Nonlinear Fiber Optics*, 3rd ed. New York: Academic, 2001.
[19] H. Chi and J. P. Yao, "Waveform distortions due to second-order dispersion and dispersion mismatches in a temporal pulse-shaping system," *J. Lightw. Technol.*, vol. 25, no. 11, pp. 3528–3535, Nov. 2007.

Ze Li received the B.S. degree in electrical engineering from Zhejiang University, Hangzhou, China, in 2007. He is currently working toward the Ph.D. degree as a joint training student at the Department of Information and Electronic Engineering, Zhejiang University, and the School of Information Technology and Engineering, University of Ottawa, Ottawa, ON, Canada.

His current research interests include microwave photonics, optical pulse processing, fiber Bragg grating based devices, and optical communications.

Hao Chi, biography not available at time of publication.

Xianmin Zhang, biography not available at time of publication.

Jianping Yao (M'99–SM'01) received the Ph.D. degree in electrical engineering in 1997 from the Université de Toulon, Toulon, France.

He joined the School of Information Technology and Engineering, University of Ottawa, Ontario, Canada, in 2001, where he is currently a Professor, Director of the Microwave Photonics Research Laboratory, and Director of the Ottawa-Carleton Institute for Electrical and Computer Engineering. From 1999 to 2001, he held a faculty position with the School of Electrical and Electronic Engineering, Nanyang Technological University, Singapore. He holds a Yongqian Endowed Visiting Chair Professorship with Zhejiang University, China. He spent three months as an invited professor in the Institut National Polytechnique de Grenoble, France, in 2005. His research has focused on microwave photonics, which includes all-optical microwave signal processing, photonic generation of microwave, mm-wave and THz, radio over fiber, UWB over fiber, fiber Bragg gratings for microwave photonics applications, and optically controlled phased array antenna. His research interests also include fiber lasers, fiber-optic sensors and bio-photonics. He is an Associate Editor of the International Journal of Microwave and Optical Technology. He is on the Editorial Board of IEEE Transactions on Microwave Theory and Techniques.

Dr. Yao received the 2005 International Creative Research Award of the University of Ottawa. He was the recipient of the 2007 George S. Glinski Award for Excellence in Research. He was named University Research Chair in Microwave Photonics in 2007. He was a recipient of an NSERC Discovery Accelerator Supplements award in 2008. Dr. Yao has authored or co-authored over 280 papers, including over 160 papers in peer-reviewed journals and 120 papers in conference proceeding. He is a registered professional engineer of Ontario. He is a fellow of the Optical Society of America and a senior member of the IEEE Photonics Society and the IEEE Microwave Theory and Techniques Society.